



Cite this: *Soft Matter*, 2020, 16, 5470

Surface enrichment of ions leads to the stability of bulk nanobubbles

Hongguang Zhang, Zhenjiang Guo and Xianren Zhang *

Numerous experiments have shown that bulk nanobubble suspensions are often characterized by a high magnitude of zeta potential. However, the underlying physical mechanism of how the bulk nanobubbles can stably exist has remained unclear so far. In this paper, based on theoretical analysis, we report a stability mechanism for charged bulk nanobubbles. The strong affinity of negative charges for the nanobubble interface causes charge enrichment, and the resulting electric field energy gives rise to a local minimum for the free energy cost of bubble formation, leading to thermodynamic metastability of the charged nanobubbles. The excess surface charges mechanically generate a size-dependent force, which balances the Laplace pressure and acts as a restoring force when a nanobubble is thermodynamically perturbed away from its equilibrium state. With this negative feedback mechanism, we discuss the nanobubble stability as a function of surface charge and gas supersaturation. We also compare our theoretical prediction with recent experimental observations, and a good agreement is found. This mechanism provides new fundamental insights into the origin of the unexplained stability of bulk nanobubbles.

Received 18th January 2020,
Accepted 10th May 2020

DOI: 10.1039/d0sm00116c

rsc.li/soft-matter-journal

1 Introduction

Nanobubbles are tiny gas-filled cavities with their typical size ranging from tens to hundreds of nanometers,^{1–3} either attached onto solid surfaces or dispersed in bulk solution. Due to their unique physicochemical characteristics, such as small size, extraordinary stability and high specific surface area,^{4,5} nanobubbles (NBs) are extensively applied in wastewater treatment, the removal of pollutants from sediments and soils, and in other environmental and biomedical applications.^{6–11} NBs can be classified into two categories based on their morphologies and locations: surface NBs and bulk NBs. Surface NBs have been widely observed on various substrates and their unexpected stability is interpreted by various theoretical models.^{12–15} Currently, three-phase contact line pinning and gas supersaturation are frequently employed to interpret the stability of surface NBs. Different from this, bulk NBs evenly disperse in bulk solution rather than sitting on solid substrates, but they also show a much longer lifetime than expected, similar to surface nanobubbles. Because of their low number density and small size, nanobubbles are difficult to detect and even harder to distinguish from other dispersed nanostructures that are assembled by amphiphilic molecules or other sources of contaminations.^{16,17} Nevertheless, the existence of bulk NBs has been claimed from various experimental observations,^{18–20} but whether they really exist

remains very controversial, as in light scattering (and also other) experiments contaminating floating bulk nanoparticles can easily be mistaken as bulk nanobubbles.^{16,21–23} Furthermore, the lack of convincing theory on nanobubble stability stirs up the controversy.

The stability of bulk nanobubbles is often correlated with the well-known phenomenon of ion enrichment at air–liquid interfaces, since the observed stable nanobubbles were frequently characterized by a high magnitude of ζ -potential (zeta potential).^{24–33} The conjecture that (both flat and curved) gas–liquid interfaces are negatively charged has been proved by accumulated experimental evidence. In 1861, Quinke observed in an electrophoresis experiment that bubbles in water migrate to the anode side,³⁴ and then Lenard reported that the interfaces between water droplets and air are negatively charged in waterfall experiments.³⁵ Since then, charging of gas/water interfaces was reported with different experimental approaches.^{36–41} In the majority of studies, surface charging was most likely due to the preferential adsorption of hydroxide ions,^{34–41} but the molecular origin of this charge remains elusive (and may even differ from case to case).^{42–45} Gray-Weale and Beattie suggested that hydroxides suppress the collective dipole-moment fluctuations of nearby water molecules,⁴² which exerts a force on the ions and attracts them to the interface region with a lower dipole-moment fluctuation. Robert showed that a region of negative charge in the interfacial layer of water, as a result of charge transfer between water molecules, gives rise to a small negative zeta potential.⁴³ Manciu and Ruckenstein explicitly accounted for the change in ion hydration between the bulk and the interface

State Key Laboratory of Organic–Inorganic Composites, Beijing University of Chemical Technology, Beijing 100029, China. E-mail: zhangxr@mail.buct.edu.cn

and obtained better agreement with experimental results.⁴⁶ The same amount of counterions is required in the diffusion layer to maintain the electroneutrality.⁴⁷

Although a high magnitude of zeta potential does lead to interparticle or interbubble repulsion and thus provides resistance against bubble coalescence,^{28,30,32,48} it is still unclear how a single charged NB can be stabilized in the presence of high Laplace pressure. Regarding the ion enrichment at air–liquid interfaces, Bunkin *et al.*^{49–51} suggested that the electrostatic pressure generated by the interaction between ions counteracts the Laplace pressure. Besides, it is demonstrated that the accumulated ions around bubble surfaces would produce a thin film, which acts as a diffusion barrier for reducing the gas dissolution, leading to a phenomenon referred to as the ion shielding effect.^{52–54} But the slowdown of gas dissolution is unlikely sufficient to interpret the long term (days or weeks) stability of charged bulk NBs. Regarding the stability of charged bulk NBs, other unsolved questions include how the solution environment (*i.e.* ionic strength, pH and dielectric double layer) and gas supersaturation affect their stability.

In this study, based on theoretical analysis, we report a stability mechanism for nanobubbles charged with negative ions. The strong affinity of the negative charges for bubble interfaces causes surface enrichment of charges and results in additional electric field energy, which in turn gives rise to a local minimum of system free energy. Mechanically, the excess surface charges generate a size-dependent coulomb force, which balances the Laplace pressure and acts as a restoring force when nanobubbles are thermodynamically perturbed away from their equilibrium state. With the negative feedback mechanism, we also compare our theoretical prediction with recent experimental data, and good agreement is found.

2 Results and discussion

2.1 Theoretical background

We considered a spherical charged NB of radius R in aqueous solution, with a volume $V = 4/3\pi R^3$ and interfacial area $A = 4\pi R^2$. In the grand canonical ensemble we adopted, the cost of grand potential for forming the pre-existing bubble, $\Delta\Omega$, includes contributions from three different origins. The first one is the volume contribution $W_V = -(p_{\text{in}} - p_{\text{out}})V$, with p_{in} and p_{out} being the pressures inside and outside the gas nanobubble. In this type of grand canonical ensemble, the chemical potential of the gas inside the bubble should be equal to that of the gas dissolved in bulk liquid. This equality is guaranteed by applying Henry's law, which gives the relationship between the pressure inside the bubble and the concentration of the dissolved gas, $p_{\text{in}} = Hc = Hc_s(1 + \xi)$, where H is the Henry coefficient, c and c_s are the actual concentration and saturation concentration of dissolved gas, and $\xi = c/c_s - 1$ is the gas supersaturation. The second term of the grand potential difference comes from the interfacial energy $W_A = \gamma A$, and the third term is the additional electrostatic potential $W_E = \frac{1}{2}\varepsilon\int_V|E|^2dV$ as a consequence of ion enrichment at the bubble interface. Here, γ is the surface tension, ε is the dielectric constant of the medium, and E is the

electric field vector. We assume that the spherical shell of nanobubbles has a uniform charge distribution, and thus the electric field vector can be written as $E = \begin{cases} 0 & r < R \\ \frac{\hat{r}Q}{4\pi\varepsilon r^2} & r \geq R \end{cases}$, in

which Q is the total amount of charges adsorbed, r is measured from the center of the bubble and \hat{r} is the unit vector in the direction of r . By combining the three contributions, the free energy cost required for generating a bulk NB is given by

$$\Delta\Omega = -[p_{\text{in}} - p_{\text{out}}]V + \gamma S + \frac{Q^2}{8\pi\varepsilon R}. \quad (1)$$

In our analysis, we assumed that the amount of surface charges at the gas–liquid interface of a bulk nanobubble remains unchanged when undergoing thermodynamic fluctuation ($R \rightarrow R + \Delta R$). This is a reasonable assumption since the characteristic time for bubble size/shape fluctuation is much shorter than that required for slow equilibrium of ion adsorption/desorption on the NB surface, especially for the solution with a small ion concentration. In determining $\Delta\Omega$ as a function of bubble radius, we set the temperature $T = 298.15$ K, $p_{\text{out}} = 1$ bar and $\gamma = 0.072$ N m⁻¹. If the solution is gas saturated, Henry's law requires $Hc_s \approx 1$ bar, whereas for the solution with stable NBs, the gas should be supersaturated and it requires $p_{\text{in}} = Hc = H(1 + \xi)c_s$.

The Poisson–Boltzmann equation was used to describe the distribution of ions around charged nanobubbles. This model assumes that surface charges are neutralized by the Stern layer and then the diffusion layer in a mean-field fashion (Fig. 1(a)). For spherical charged bubbles, the Poisson–Boltzmann equation can be written as²⁰ $\frac{d^2\psi(x)}{dx^2} + 2/(R+x)\frac{d\psi(x)}{dx} = \frac{2}{\varepsilon_r\varepsilon_0}Ze\rho_{\text{bulk}}\sinh\left[\frac{Ze}{k_B T}\psi(x)\right]$, where ε_r is the relative dielectric constant of water (80 at room temperature), ε_0 is the dielectric permittivity of vacuum (8.854×10^{-12} C V m⁻¹), Z is the ionic valence, e is the electronic charge (1.602×10^{-19} C), ρ_{bulk} is the concentration of ions in the bulk solution (ions per m³), k_B is the Boltzmann constant, and $\psi(x)$ is the electric potential at a distance x from the charged surface. It is worth mentioning that here we only considered the monovalent electrolyte solution, such as NaCl. According to Debye and Huckel⁵⁵ and Ohshima *et al.*⁵⁶ the surface charge density can be determined by

$$\sigma_0 = Z\sqrt{2\varepsilon_r\varepsilon_0k_B T\rho_{\text{bulk}}} \times \left[2\sinh\left(\frac{e\psi_0}{2k_B T}\right) + \frac{4}{R\left(\frac{\varepsilon_0\varepsilon_r k_B T}{2e^2 Z^2 \rho_{\text{bulk}}}\right)^{-1/2}} \tanh\left(\frac{e\psi_0}{4k_B T}\right) \right] \quad (2)$$

Here, the zeta potential ζ is assumed to be equal to the Stern potential ψ_{stern} . The surface potential can be expressed as $\psi_0 = \psi_{\text{drop}} + \zeta$, where the Stern layer can be assumed to act as a parallel concentric sphere capacitor⁵⁷ and the potential drop ψ_{drop} is assumed to be linear within the Stern layer. Thus, $\psi_{\text{drop}} = \frac{d_{\text{stern}}\sigma_0}{\varepsilon_r\varepsilon_0}$

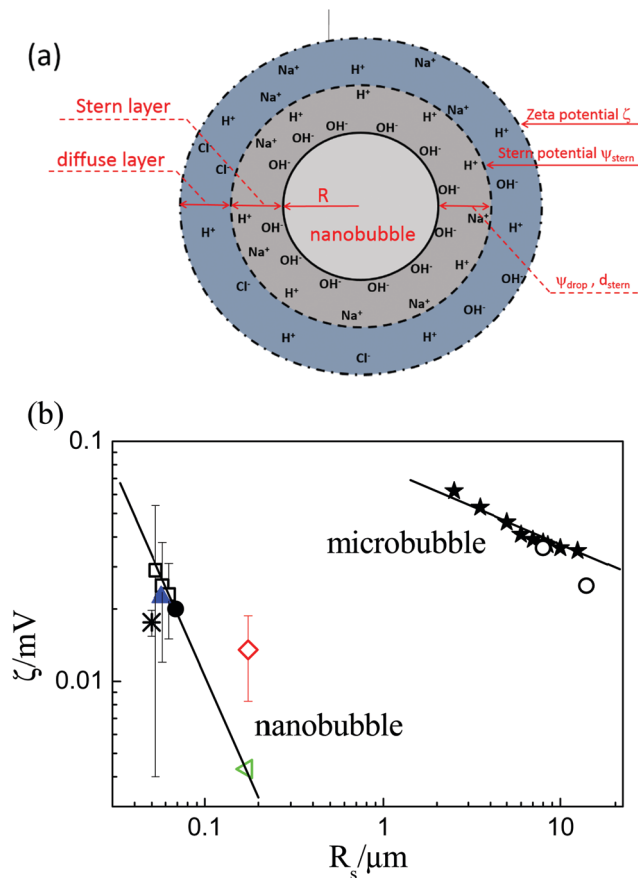


Fig. 1 (a) Schematic illustration of the electrical double layer formed around a charged nanobubble. (b) Experimental data summarized for stable bulk nanobubbles^{24,26,30,63,64} and microbubbles^{65,66} in deionized water. In this figure, the power law relationship between ζ and R_s is also given.

with d_{stem} being the width of the Stern layer (see Fig. 1(a)). Within the Debye–Hückel approximation, the relationship between the charge density and zeta potential can be simplified as⁵⁸

$$\sigma_0 = \frac{Q}{A} = \frac{\varepsilon_r \varepsilon_0 \zeta}{\lambda_D} \quad (3)$$

where λ_D is the Debye length (0.6 nm for pure water). Note that the model of Stern layer and diffuse layer has been used here without taking ionic specificity into account.^{28,59,60} However, the mechanism would still hold if other surface force models are employed since the proposed mechanism is essentially based on zeta potential (eqn (3)), rather than the detailed local ion distribution on bubble surfaces (eqn (2)).

2.2 Stability mechanism for a single charged bulk nanobubble

The classical DLVO theory, which was established by Derjaguin, Landau, Verwey and Overbeek,^{61,62} is a classical theory to explain the stability of colloids by considering both the attractive van der Waals force and the repulsive electric double layer force. For neighboring nanobubbles with electrically charged interfaces, the overlap of the double layers belonging to neighboring

NBs produces electrostatic repulsion,^{27,28} thus inhibiting NB coalescence or aggregation. However, for a single bulk NB, it remains unclear why the bubble is stable and how the surface charge enrichment and gas supersaturation are coupled together to affect the behavior of bubbles.

2.2.1 The power law relationship between ζ and bubble radius R_s as well as the curvature dependence of adsorbed negative charges. In this study we assume that the mechanical equilibrium of nanobubbles can be reached much faster than the settlement of chemical equilibrium of ions, *i.e.*, the ion enrichment at the bubble interface is governed by the slower dynamics of ion adsorption and desorption. This leads us to assume that the amount of surface charges at the gas–liquid interface of a bulk nanobubble in equilibrium with the surrounding remains unchanged, even if it undergoes rapid thermodynamic fluctuations. This assumption seems also to be consistent with the experimental observations that stable nanobubbles exist under different conditions (see Fig. 1(b)).

In Fig. 1(b) we summarize the recent experimental results of the measured zeta potential and bubble size, for both nanobubbles and microbubbles. Note that we only displayed the data in deionized water, and hence $\sigma \equiv \sigma_{\text{flat}}(c_{\text{H}^+}, c_{\text{OH}^-}, c_{\text{Na}^+}, c_{\text{Cl}^-})$ is constant. The figure clearly demonstrates that ζ and R_s (R_s the bubble radius) roughly satisfy a power law relationship. The relationship can be interpreted with eqn (3). Here the charge density on a bubble surface is considered as $\sigma_0 = \sigma_{\text{flat}}(1 + f_R(R_s))$, which depends on the solution properties of charge distribution (namely, the charge density at a flat air–liquid interface $\sigma_{\text{flat}}(c_{\text{H}^+}, c_{\text{OH}^-}, c_{\text{Na}^+}, c_{\text{Cl}^-})$) and the curvature correction $f_R(R_s)$ for the effect of curvature of bubble interfaces. Here $f_R(R_s)$ is a dimensionless variable. Combining $Q = A \cdot \sigma_{\text{flat}}(1 + f_R(R_s))$ and eqn (3) leads to $\log_{10}(1 + f_R(R_s)) + \log_{10}\left(\frac{\sigma_{\text{flat}} \lambda_D}{\varepsilon_r \varepsilon_0} \cdot \frac{1}{\zeta}\right) = 0$.

With this power law relationship (Fig. 1(a)), fitting the experimental data of microbubbles in deionized water^{65,66} leads to a rate of $R_s^{-0.38}$ for the decay of $1 + f_R(R_s)$ as the bubble radius increases. Another consequence of the power law fitting is that the intercept on the y -axis is $\frac{\sigma_{\text{flat}} \lambda_D}{\varepsilon_r \varepsilon_0}$ (namely, $1 + f_R = 1$ or $\log_{10}(1 + f_R) = 0$ for $R_s \rightarrow \infty$), from which we obtained $\sigma_{\text{flat}} = -0.0028 \text{ C m}^{-2}$. With the given σ_{flat} along with the experimental data for nanobubbles in deionized water (see Table 1), we can roughly determine R_s^{-2} for nanobubbles.

2.2.2 Metastability of charged nanobubbles. We then investigated the ion-enrichment effect on the free energy cost for bulk NB formation by analyzing eqn (1). The numerically determined $\Delta\Omega$ is shown in Fig. 2(a) as a function of bubble radius. The figure indicates that for a NB with a constant surface charge (here we chose $Q = -2.3456 \times 10^{-15} \text{ C}$ as an example), three different situations appear according to eqn (1). The first scenario, *e.g.* at a given gas supersaturation of $\zeta = 8$ (see the short dashed line in Fig. 2(a)), is characterized by a monotonic decrease of $\Delta\Omega$. In this case, NBs become unstable and will grow spontaneously from the initial size. At moderate gas supersaturation ($0 < \zeta < 8$), however, the free energy profile ceases to monotonically decrease and displays two

Table 1 Summary of recent experimental data on nanobubbles and microbubbles as well as the charge density estimated by employing eqn (2)

pH range	Ionic strength (M)	Gas type	Bubble radius ^a (nm)	Zeta potential ^a (mV)	Charge density ^b (C m ⁻²)	Ref.
7	0	Ozone/oxygen	257 ± 41/89.5 ± 41	-39.5 ± 3.8/-20.1 ± 5.4	-0.0302/-0.0217	Meegoda <i>et al.</i> 2018 ²⁴
	0.01 NaCl		253.5 ± 15.5/107 ± 44.5	-28.6 ± 1.2/-21.6 ± 3.9	-0.0244/-0.0231	
	0.1 NaCl		246.5 ± 47.5/95 ± 17	-20.2 ± 0.3/-13.6 ± 4.5	-0.214/-0.0235	
	1 NaCl		340 ± 17.5/110 ± 64	-11.6 ± 1.2/-11.1 ± 2.8	-0.0139	
	0.002 NaCl	Ozone	74 ± 31	-27 ± 4.2	-0.0275	
		Oxygen	56.7 ± 23	-22.4 ± 3.4	-0.0203	
		Air	56.2 ± 46	-21.3 ± 3	-0.0299	
		Nitrogen	51.1 ± 32	-19.8 ± 5.3	-0.0280	
		Oxygen	172 ± 17	-4.3 ± 0.3	-0.0031	
4	0		89.5 ± 41	-20.1 ± 5.4	-0.0181	
7			41.5 ± 11.5	-27.3 ± 3.2	-0.0240	
10			68.5	-17 to -20	-0.0216	Ushikubo <i>et al.</i> 2010 ³⁰
5.7-6.2	0	Air	50-500	-34 to -45	-0.03342	Uchida <i>et al.</i> 2011 ⁶³
6.2-6.4	0	Oxygen	60-250	-22	-0.0169	Zheng <i>et al.</i> 2015 ⁶⁴
7	0	Ozone	80-170	-27 to -45	-0.0299	Ahmed <i>et al.</i> 2018 ²⁶
7	0	Oxygen/Nitrogen/Air	2500-12 500/8500-27 500	-35 to -62/-28 to -42		Takahashi <i>et al.</i> 2005/2007 ^{65,66}
7	0	Air/Carbon dioxide	300-225	-13	-0.0139	Bui <i>et al.</i> 2019 ⁶⁷
4-12	0.001 NaCl	Air				

^a Experimentally measured value from the literature. ^b Calculated value by using eqn (2).

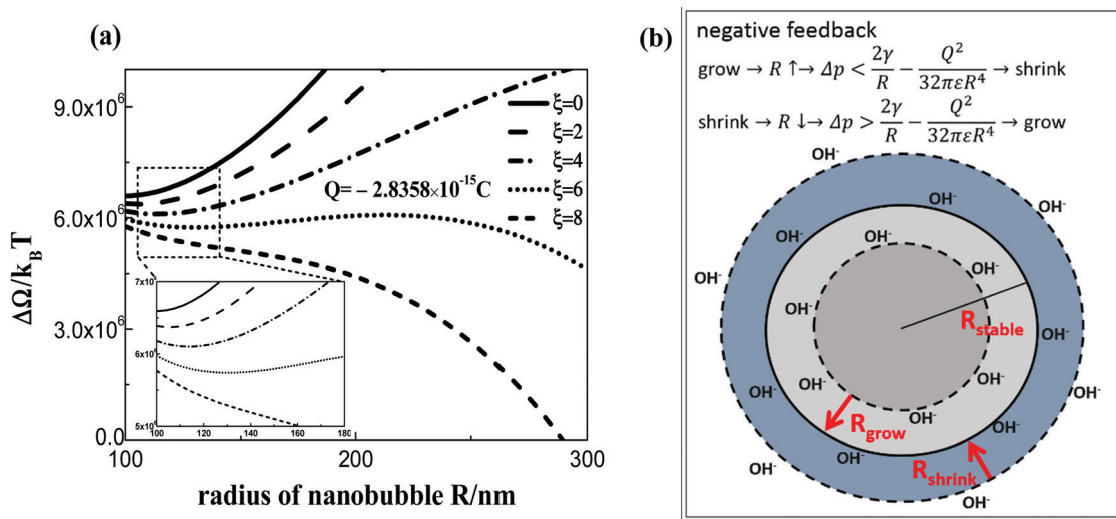


Fig. 2 (a) The required free energy cost for producing a tiny bubble as a function of bubble radius, under the conditions of fixed charge enrichment. (b) The schematic illustration of the negative feedback mechanism for stabilizing a bulk nanobubble with the constant adsorption of hydroxide ions onto the bubble interface.

equilibrium states. One is a maximum that represents an unstable state although the bubble is in equilibrium with the solvent, whereas the other corresponds to a local minimum of the free energy cost, which clearly indicates the metastability of the nanobubble. The third case is that there is only one maximum value of free energy cost as the radius varies (e.g., $\xi = 0$, which is not fully shown in Fig. 2(a)), indicating that the NB is again in an unstable state, and thus the nanobubble in equilibrium with the surrounding would either shrink or continue to grow under a small thermodynamic perturbation.

Importantly, Fig. 2(a) clearly indicates that at a certain range of gas supersaturation, a charged bulk NB can be thermodynamically stable (in fact metastable) in an open system. Thus, we concluded that the excess adsorption of negative charges on the NB surfaces may lead to the stability of bulk NBs in a gas supersaturated solution ($\xi > 0$).

2.2.3 Negative feedback mechanism and the restoring force. In this section, we analyze, from the mechanical view of point, how excess surface charge and gas supersaturation govern the nanobubble stability. Fig. 2(b) gives the mechanism of how bulk NBs respond to their size variation under thermodynamic fluctuation. The mechanical equilibrium for a NB can be obtained by setting $\frac{\partial\Delta\Omega}{\partial R} = 0$, which leads to $p_{\text{in}} + \frac{Q^2}{32\pi^2\epsilon R^4} = p_{\text{out}} + \frac{2\gamma}{R}$, similar to that argued by Boshenyatov *et al.*,²⁷ Yasui *et al.*³³ and Ahmed *et al.*²⁶ This relationship can be interpreted in a manner of mechanical equilibrium (see Fig. 2(b)), namely, at equilibrium the expanding forces on the left-hand side ($f_{\text{expanding}} \equiv p_{\text{in}} + \frac{Q^2}{32\pi^2\epsilon R^4}$) need to balance the collapsing forces on the right-hand side ($f_{\text{collapsing}} \equiv p_{\text{out}} + \frac{2\gamma}{R}$). This leads to a negative feedback mechanism. If the bubble initially grows,

electrostatic effects $\frac{Q^2}{32\pi^2\epsilon R^4}$ will decay faster than Laplace pressure $\frac{2\gamma}{R}$ (under conditions that Q remains constant or changes more weakly than $1/R$). This leads to $f_{\text{expanding}} < f_{\text{collapsing}}$ and thus the bubble will shrink back to the equilibrium state (Fig. 2(b)). Conversely, the shrinking of the bubble size would lead to a preponderance of the expanding forces, *i.e.*, $f_{\text{expanding}} > f_{\text{collapsing}}$, and as a result the bubble will expand to its equilibrium size (Fig. 2(b)). In summary, under conditions that Q remains constant or changes more weakly than the bubble size, the electrostatic effect acts as a restoring force to stabilize nanobubbles, which prevents the nanobubbles in equilibrium from shrinking and growing.

2.3 Nanobubble stability as a function of surface charge and gas supersaturation

Within the framework of the above-proposed interface restoration model, we then investigated, by analyzing eqn (1), how the stability of bulk nanobubbles depends on gas supersaturation and the amount of surface charges adsorbed. For this purpose, we need first to determine the possible range of σ and Q , in which nanobubbles remain stable. According to the experimental data for which stable nanobubbles exist (see those summarized in Table 1), we estimated the surface charge density σ and surface charge Q in different solution environments (such as at different pH values and ion strength) through eqn (2). This gives the range of charge density as well as surface charge quantities for stable NBs: $\sigma \in (-0.0022 \text{ C m}^{-2}, -0.036 \text{ C m}^{-2})$ and $Q \in (-0.8 \times 10^{-15} \text{ C}, -5.2 \times 10^{-15} \text{ C})$. This range of surface charge density was fully covered while searching for stable nanobubbles during the following theoretical analysis.

The effect of the amount of adsorbed charges on bubble stability is shown in Fig. 3. According to the thermodynamic analysis on the determined free energy profile, as demonstrated in the inset of Fig. 3(a), stable NBs only exist within a certain range of gas supersaturation (see the shaded region in Fig. 3(a)). Increasing the amount of surface charges reduces both the upper and lower limits of gas supersaturation needed

for stabilizing a NB. But the upper limit decreases more sharply, leading to a decreasing range of gas supersaturation for forming stable nanobubbles (see Fig. 3(a)). Note that the upper limit of gas supersaturation for stable NBs was determined at which the local minimal of free energy cost disappears. Here we need to particularly explain how to determine the lower limits. Taking derivative of eqn (1) yields $\frac{\partial \Omega}{\partial R} = -\Delta p \frac{dV}{dR} + 8\pi R \left(\gamma - \frac{Q^2}{64\pi^2\epsilon R^3} \right)$.

This equation indicates that $\gamma - \frac{Q^2}{64\pi^2\epsilon R^3} \geq 0$ should be satisfied in order to balance Δp . Therefore, this gives the lower limit of the radius, $R \geq \sqrt[3]{\frac{Q^2}{64\gamma\pi^2\epsilon}}$, and this inequality also determines the lower limit of gas supersaturation.

Fig. 3(b) shows the relationship between the radius of the stable nanobubbles and the gas supersaturation, as a function of the amount of excess surface charges. Under certain gas supersaturation, such as $\xi = 1$, increasing the amount of excess charges will cause a nearly linear increase of the radius of stable bubbles. On the other hand, at a given surface charge, the radius of the resulting stable NBs increases with gas supersaturation (Fig. 3(b)). This interplay between gas supersaturation and excess surface charge is explained as follows. When the gas supersaturation increases, $\Delta p = Hc_s\xi > \frac{2\gamma}{R}$, namely $f_{\text{expanding}} > f_{\text{collapsing}}$, which causes the increase of the size of stable nanobubbles. This agrees with the change of the free energy cost: as the level of gas supersaturation increases, the energy barrier for bubble growth will gradually decrease (Fig. 2(a)) until it finally disappears, causing the nanobubbles to come into the unstable regime. Similarly, increasing the surface charge leads to the same tendency in the change of nanobubble states. In general, Fig. 3(b) again indicates the effect of cooperative interplay between the electric field and gas supersaturation on the stability of nanobubbles.

2.4 Discussion on experimental data for bulk nanobubbles

Experimental studies always related the stability of bulk NBs to the large magnitude of the measured zeta potential. To discuss the experimental data, here we first performed a theoretical

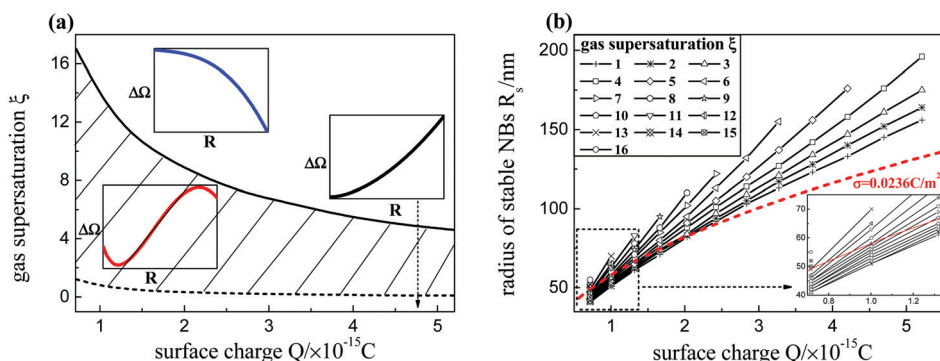


Fig. 3 Nanobubble stability determined from free energy analysis (eqn (1)). (a) The range of bulk nanobubbles in different states, either stable or unstable, as a function of gas supersaturation and the amount of surface charges. The insets show the corresponding free energy profile as a function of bubble radius in three regions, indicating various degrees of bubble stability. (b) The radius of stable nanobubbles as a function of the amount of excess surface charges, under different levels of gas supersaturation. The dashed line (red) in the figure represents a constant charge density of 0.0236 C m^{-2} .

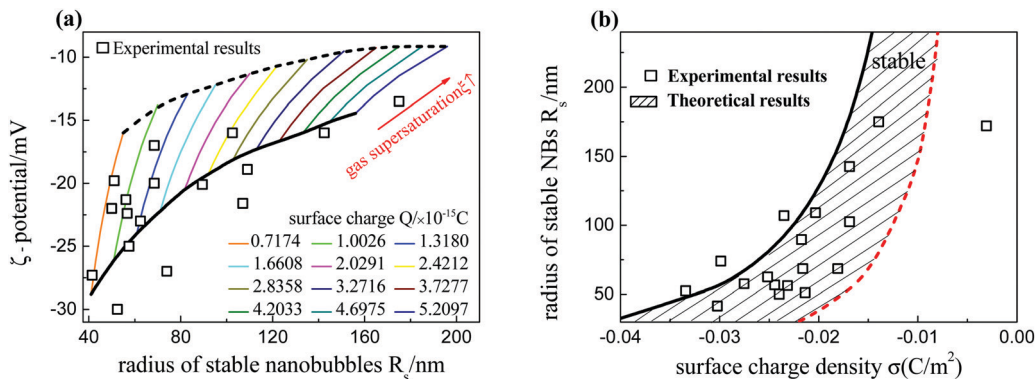


Fig. 4 Comparison of theoretical analysis and experimental data (square symbols). (a) Relationship between bubble radius and zeta potential under different amounts of charges adsorbed and gas supersaturation. The theoretical results from free energy analysis are the same as in Fig. 3(b), while the amounts of charges were replaced by zeta potential through eqn (3). The upper dashed line and the lower solid line give stability boundaries. (b) Relationship between bubble radius and charge density, in which the calculated range of stable nanobubbles (the shadowed region) was determined by setting the range of surface charge density to $\sigma \in (-0.0022 \text{ C m}^{-2}, -0.036 \text{ C m}^{-2})$ (the range is estimated from the experimental data shown in Table 1). In this figure experimental data for stable nanobubbles (square symbols) were also shown for a comparison. As listed in Table 1, the experimental data are from ref. 24, 26, 30, 63, 64 and 67.

analysis on the relationship between the radius and zeta potential of stable nanobubbles (see Fig. 4(a)), under different levels of charges adsorbed and gas supersaturation. We predict, as shown in this figure, that as the nanobubble radius increases, both the upper and lower limits of zeta potentials required for the existence of stable NBs gradually increase. Note that in this figure the zeta potential was determined through eqn (3), while the lower limit of the radius was determined

according to $R \geq \sqrt[3]{\frac{Q^2}{64\gamma\pi^2\epsilon}}$, as discussed above.

The experimental data are also shown in Fig. 4(a), in comparison with the range of nanobubble stability from our theoretical prediction. Note that in the theoretical prediction we have set the Debye length and relative dielectric constant of pure water to 0.6 nm and 80 for determining ζ -potential with eqn (3). In general, the qualitative agreement with experimental results indicates that the present mechanism provides qualitative criteria to answer the question of why bulk NBs can survive for a long time. We also need to point out that although qualitative agreement is achieved between the experimental data and our calculations, the theoretically predicted region for stable nanobubbles cannot completely cover the range of experimental data in which stable nanobubbles were reported. Interpretation of the difference requires accounting for several neglected effects. These include the variation of surface tensions due to the surface adsorption of impurities, and the ion dependent surface adsorption,^{28,68,69} and other unknown reason factors.

In the above discussion we do not consider the effect of the solution environment on surface charge density. In fact, the solution properties, especially the pH value, ion concentration and dielectric constant, strongly affect the regulation of surface charges.^{24,26,32} As discussed in Section 2.2.1, when the solution pH, ion concentration and species remain unchanged, the adsorption amount of charges per unit gas-liquid interface (surface density for charges adsorbed) remains roughly constant with a curvature correction $\sigma = \sigma_{\text{nat}}(c_{\text{H}^+}, c_{\text{OH}^-}, c_{\text{Na}^+}, c_{\text{Cl}^-})(1 + f_R)$. The dashed line in

Fig. 3(b) represents a constant charge density (depending on the nature of the solution, namely, $\sigma_{\text{nat}}(c_{\text{H}^+}, c_{\text{OH}^-}, c_{\text{Na}^+}, c_{\text{Cl}^-})$), by ignoring its dependence on bubble radius and setting $f_R(R) = 0$. Therefore, the size of stable nanobubbles is in fact determined by the intersection of the solid line (which represents the effect of given gas supersaturation) and the dashed line (which represents the effect of solution environment on the enrichment of adsorbed charges). According to the calculation results summarized in Table 1, the charge density estimated from experimental data varies from $\sigma = -0.0022$ to -0.036 C m^{-2} . Within the given range of surface density, we can determine the region in which stable nanobubbles exist.

Fig. 4(b) summarizes the theoretical prediction and the experimental data listed in Table 1. Apparently, the experimental data are basically located within the shaded area predicted by our analysis. The agreement in turn proves that our theoretical analysis considers the main factors affecting the bubble stability. But we need to point out again that there are several experimental data out of our region of theoretical prediction. It means that this mechanism alone is unable to interpret all experimental results and there must exist other mechanisms for nanobubble stability.

3 Conclusions

For nanobubbles dispersed in bulk liquid, it is often found that they can survive with an unexpected long lifetime of days or weeks. It is generally considered that the high magnitude of zeta potential of bulk nanobubbles is related to their stability, while the underlying physical mechanism is currently unknown. In this paper, based on theoretical analysis, we report the stability mechanism of bulk nanobubbles, the surfaces of which are negatively charged. Our model demonstrates that for nanobubbles of a given size, the electric field energy generated by the excess and strong adsorption of hydroxides will induce a local minimum of system free energy, leading to thermodynamic

metastability of the charged nanobubbles. The excess surface charges mechanically generate a size-dependent force, which balances the Laplace pressure and acts as a restoring force when the nanobubble is thermodynamically perturbed away from its equilibrium state. With the negative feedback mechanism, we analyzed the effect of cooperative interplay between the electric field and gas supersaturation on the stability of nanobubbles.

Finally, we discussed the agreement and disagreement between our theoretical prediction and experimental observations. Basically, the experimental data are located within the region predicted by our analysis, indicating that the mechanism provides insights into the origin of unexplained stability for bulk nanobubbles. However, there are still several experimental data out of our region of theoretical prediction, meaning that there must exist other mechanisms for nanobubble stability.

Conflicts of interest

There are no conflicts to declare.

Acknowledgements

This research was supported by the National Natural Science Foundation of China (No. 21978007).

References

- 1 T. Uchida, S. Oshita, M. Ohmori, T. Tsuno, K. Soejima, S. Shinozaki, Y. Take and K. Mitsuda, *Nanoscale Res. Lett.*, 2011, **6**, 2–9.
- 2 W. B. Zimmerman, V. Tesař and H. C. H. Bandulasena, *Curr. Opin. Colloid Interface Sci.*, 2011, **16**, 350–356.
- 3 K. Ulatowski, P. Sobieszuk, A. Mróz and T. Ciach, *Chem. Eng. Process.*, 2019, **136**, 62–71.
- 4 D. Lohse and X. Zhang, *Rev. Mod. Phys.*, 2015, **87**, 981.
- 5 M. Chaplin, 2017, www1.lsbu.ac.uk/water/nanobubble.html.
- 6 A. Agarwal, W. J. Ng and Y. Liu, *Chemosphere*, 2011, **84**, 1175.
- 7 L. Hu and Z. Xia, *J. Hazard. Mater.*, 2018, **342**, 446.
- 8 J. N. Meegoda, J. H. Batagoda and S. Aluthgun-Hewage, *Environ. Eng. Sci.*, 2017, **12**, 1.
- 9 D. Narayan, 2017, www.biotecharticles.com/Nanotechnology-Article/Development-and-Applications-of-Nanobubbles-3129.html.
- 10 S. Liu, S. Oshita, Y. Makino, Q. Wang, Y. Kawagoe and T. Uchida, *ACS Sustainable Chem. Eng.*, 2015, **4**, 1347.
- 11 E. Y. Lukianova-Hleb, A. Belyanin, S. Kashinath, X. Wu and D. O. Lapotko, *Biomaterials*, 2012, **33**, 1821.
- 12 J. R. Seddon, D. Lohse, W. A. Ducker and V. S. Craig, *ChemPhysChem*, 2012, **13**, 2179–2187.
- 13 Y. Liu and X. Zhang, *J. Chem. Phys.*, 2014, **141**, 134702.
- 14 Y. Liu and X. Zhang, *J. Chem. Phys.*, 2013, **138**, 014706.
- 15 D. Lohse and X. Zhang, *Phys. Rev. E: Stat., Nonlinear, Soft Matter Phys.*, 2015, **91**, 031003(R).
- 16 M. Alheshibri and V. S. J. Craig, *J. Colloid Interface Sci.*, 2019, **542**, 136–143.
- 17 A. J. Jadhav and M. Barigou, *Langmuir*, 2020, **36**, 1699–1708.
- 18 N. F. Bunkin, A. V. Shkirin, I. S. Burkhanov, L. L. Chaikov and A. K. Lomkova, *Quantum Electron.*, 2014, **44**, 1022.
- 19 F. Jin, J. Li, X. Ye and C. Wu, *J. Phys. Chem. B*, 2007, **111**, 11745.
- 20 K. Ohgaki, N. Q. Khanh, Y. Joden, A. Tsuji and T. Nakagawa, *Chem. Eng. Sci.*, 2010, **65**, 1296.
- 21 M. Sedlak and D. Rak, *J. Phys. Chem. B*, 2013, **117**, 2495–2504.
- 22 D. Rak, M. Ovadova and M. Sedlak, *J. Phys. Chem. Lett.*, 2019, **10**, 4215–4221.
- 23 F. Jin, J. Ye, L. Hong, H. Lam and C. Wu, *J. Phys. Chem. B*, 2007, **111**, 2255–2261.
- 24 J. N. Meegoda, S. H. Hewage and J. H. Batagoda, *Environ. Eng. Sci.*, 2018, **35**, 1216–1227.
- 25 S. I. Koshoridze and Y. K. Levin, *Tech. Phys. Lett.*, 2018, **44**, 1245–1247.
- 26 A. Khaled Abdella Ahmed, C. Sun, L. Hua, Z. Zhang, Y. Zhang, T. Marhaba and W. Zhang, *Environ. Eng. Sci.*, 2018, **35**, 720–727.
- 27 B. V. Boshenyatov, S. I. Kosharidze and Yu. K. Levin, *Russ. Phys. J.*, 2019, **61**, 1914–1921.
- 28 J. N. Meegoda, S. A. Hewage and J. H. Batagoda, *Langmuir*, 2019, **35**, 12100–12112.
- 29 J. K. Beattie, A. M. Djerdjev, A. Gray-Weale, N. Kallay, J. Lützenkirchen, T. Preočanin and A. Selmani, *J. Colloid Interface Sci.*, 2014, **422**, 54–57.
- 30 F. Y. Ushikubo, T. Furukawa, R. Nakagawa, M. Enari, Y. Makino, Y. Kawagoe, T. Shiina and S. Oshita, *Colloids Surf., A*, 2010, **361**, 31–37.
- 31 S. O. Yurchenko, A. V. Shkirin, B. W. Ninham, A. A. Sychev, V. A. Babenko, N. V. Penkov, N. P. Kryuchkov and N. F. Bunkin, *Langmuir*, 2016, **32**, 11245–11255.
- 32 N. Nirmalkar, A. W. Pacek and M. Barigou, *Soft Matter*, 2018, **14**, 9643–9656.
- 33 K. Yasui, T. Tuziuti and W. Kanematsu, *Ultrason. Sonochem.*, 2018, **48**, 259–266.
- 34 G. Quinke, *Annu. Rev. Phys. Chem.*, 1861, **113**, 513–598.
- 35 P. Lenard, *Ann. Phys.*, 1892, **46**, 584–636.
- 36 K. A. Karraker and C. J. Radke, *Adv. Colloid Interface Sci.*, 2002, **96**, 231–264.
- 37 C. Yang, T. Dabros, D. Li, J. Czarnecki and J. H. Masliyah, *J. Colloid Interface Sci.*, 2001, **243**, 128–135.
- 38 M. Takahashi, *J. Phys. Chem. B*, 2005, **109**, 21858–21864.
- 39 K. Ciunel, M. Armélin, G. H. Findenegg and R. V. Klitzing, *Langmuir*, 2005, **21**, 4790–4793.
- 40 P. Creux, J. Lachaise, A. Graciaa and J. K. Beattie, *J. Phys. Chem. C*, 2007, **111**, 3753–3755.
- 41 A. Graciaa, P. Creux and J. Lachaise, *Surfactant Sci. Ser.*, 2002, **106**, 825–836.
- 42 A. Gray-Weale and J. K. Beattie, *Phys. Chem. Chem. Phys.*, 2009, **11**, 10994.
- 43 C. J. Mundy, I. F. W. Kuo, M. E. Tuckerman, H. S. Lee and D. J. Tobias, *Chem. Phys. Lett.*, 2009, **481**, 2–8.
- 44 R. Vacha, Q. Marsalek, A. P. Willard, D. J. Bonhuis, R. R. Netz and P. Jungwirth, *J. Phys. Chem. Lett.*, 2011, **3**, 107–111.
- 45 M. D. Baer, I. F. W. Kuo, D. J. Tobias and C. J. Mundy, *J. Phys. Chem. B*, 2014, **118**, 8364–8372.

- 46 M. Manciu and F. Ruckenstein, *Adv. Colloid Interface Sci.*, 2003, **105**, 63–101.
- 47 J. K. Beattie, A. M. Djerdjev and G. G. Warr, *Faraday Discuss.*, 2009, **141**, 81–98.
- 48 S. H. Oh and J. M. Kim, *Langmuir*, 2017, **33**, 3818–3823.
- 49 S. O. Yurchenko, A. V. Shkirin, B. W. Ninham, A. A. Sychev, V. A. Babenko, N. V. Penkov, N. P. Kryuchkov and N. F. Bunkin, *Langmuir*, 2016, **32**, 11245–11255.
- 50 N. F. Bunkin, A. V. Shkirin, N. V. Suyazov, V. A. Babenko, A. A. Sychev, N. V. Penkov, K. N. Belosludtsev and S. V. Gudkov, *J. Phys. Chem. B*, 2016, **120**, 1291–1303.
- 51 N. F. Bunkin and A. V. Shkirin, *J. Chem. Phys.*, 2012, **137**, 054707.
- 52 E. Dressaire, R. Bee, D. C. Bell, A. Lips and H. A. Stone, *Science*, 2008, **320**, 1198–1201.
- 53 T. Uchida, S. Liu, M. Enari, S. Oshita, K. Yamazaki and K. Gohara, *Nanomaterials*, 2016, **6**, 31.
- 54 J. H. Weijs, J. R. T. Seddon and D. Lohse, *ChemPhysChem*, 2012, **13**, 2197–2204.
- 55 P. Debye and E. Hückel, *Phys. Z.*, 1923, **24**, 742.
- 56 H. Ohshima, T. W. Healy and L. R. White, *J. Colloid Interface Sci.*, 1982, **90**, 17–26.
- 57 E. J. W. Verwey and J. T. G. Overbeek, *J. Colloid Sci.*, 1955, **10**, 224–225.
- 58 H. J. Butt, K. Graf and M. Kappl, *Physics and Chemistry of Interfaces*, Wiley-VCH, Weinheim, Germany, 2006, ISBN: 9783527406296.
- 59 V. S. J. Craig, B. W. Ninham and R. M. Pashley, *Nature*, 1993, **364**, 317–319.
- 60 B. W. Ninham, R. M. Pashley and P. L. Nostro, *Curr. Opin. Colloid Interface Sci.*, 2017, **27**, 25–32.
- 61 F. L. Leite, C. C. Bueno, A. L. Da Roz, E. C. Ziemath and O. N. Oliveira, *Int. J. Mol. Sci.*, 2012, **13**, 12773–12856.
- 62 V. Uskokovic, *J. Dispersion Sci. Technol.*, 2012, **33**, 1762–1786.
- 63 T. Uchida, S. Oshita, M. Ohmori, T. Tsuno, K. Soejima, S. Shinozaki, Y. Take and K. Mitsuda, *Nanoscale Res. Lett.*, 2011, **6**, 1.
- 64 T. L. Zheng, Q. H. Wang, T. Zhang, Z. N. Shi, Y. L. Tian, S. S. Shi, N. Smale and J. Wang, *J. Hazard. Mater.*, 2015, **287**, 412–420.
- 65 M. T. Takahashi, *J. Phys. Chem. B*, 2005, **109**, 21858–21864.
- 66 M. T. Takahashi, K. Chiba and P. Li, *J. Phys. Chem. B*, 2007, **111**, 1343–1347.
- 67 T. T. Bui, D. C. Nguyen and M. Han, *J. Nanopart. Res.*, 2019, **21**, 173.
- 68 Z. J. Guo, X. Wang and X. R. Zhang, *Langmuir*, 2019, **35**, 8482–8489.
- 69 A. A. Atchley, *J. Acoust. Soc. Am.*, 1989, **85**, 152–157.